



Article

Bituminous Coal Sorption Characteristics and Its Modeling of the Main Coal Seam Gas Component in the Huabei Coalfield, China

Gang Wu ^{1,2}, Zhiwei Ye ^{1,3}, Lei Zhang ^{1,2,*} and Jun Tang ⁴

¹ School of Mines, China University of Mining and Technology, Xuzhou 221116, China; wu007gang007@cumt.edu.cn (G.W.)

² Guizhou Mine Safety and Energy Innovation Technology Co., Ltd., Guiyang 550025, China

³ Institute of Resources and Environment, Henan Polytechnic University, Jiaozuo 454000, China

⁴ School of Safety Engineering, China University of Mining and Technology, Xuzhou 221116, China

* Correspondence: zhang_lei@cumt.edu.cn; Tel.: +86-187-9620-415

Abstract: Knowledge of the gas sorption and permeability characteristics of a coal provides an essential basis for the evaluation of coalbed methane reserves and their recoverability. Thus, the gas excess sorption capacities of the main gas component of coal seam gas (CSG) in bituminous coal samples derived from the Xutuan Coal Mine in the Huabei Coalfield, in the Anhui Province of China, were measured using a volumetric method. The results showed that under the same equilibrium pressure, the order of excess sorption capacity was $\text{CO}_2 > \text{CH}_4 > \text{N}_2$. Furthermore, the sorption capacity ratios of coal from the Xutuan Mine for CO_2 , CH_4 , and N_2 were approximately 6.0:2.3:1. It was also demonstrated that the sorption capacity during depressurization was always larger than that of the adsorption process, which is indicative of desorption hysteresis. The behaviors of three adsorption models, Langmuir, BET, and D-R, all of which include two parameters, are considered in this paper. The different gas sorption measurement data were fitted by the three models. For the bituminous coal samples, the fits of the D-R equation of all three different gases are higher than 0.99, the fits of the Langmuir equation are higher than 0.985, while the fits of the BET equation for CH_4 and N_2 absorption are higher than 0.95. However, the fits of the BET equation for CO_2 absorption are only about 0.5. Coal sorption has an apparent influence on coal permeability; the permeability of the same coal sample to N_2 , CH_4 , and CO_2 gases was tested and analyzed. The result shows that the permeability of CO_2 was found to be lower than that of other coal seam gas constituents, CH_4 and N_2 , due to their different adsorption abilities.

Keywords: coal seam gas; coal permeability; gas sorption capacity; volumetric method; adsorption models



Citation: Wu, G.; Ye, Z.; Zhang, L.; Tang, J. Bituminous Coal Sorption Characteristics and Its Modeling of the Main Coal Seam Gas Component in the Huabei Coalfield, China. *Sustainability* **2023**, *15*, 9822.

<https://doi.org/10.3390/su15129822>

Academic Editors: Chaolin Zhang and Jianjun Ma

Received: 29 May 2023

Revised: 17 June 2023

Accepted: 18 June 2023

Published: 20 June 2023



Copyright: © 2023 by the authors. Licensee MDPI, Basel, Switzerland. This article is an open access article distributed under the terms and conditions of the Creative Commons Attribution (CC BY) license (<https://creativecommons.org/licenses/by/4.0/>).

1. Introduction

Coal seam gas (CSG), or coalbed methane (CBM), as an important source of unconventional energy, is increasingly becoming an essential methane supply resource. CSG consists mainly of methane (CH_4) (more than 90%) and is used as a low emission alternative for energy production [1]. CBM is stored primarily in coal through adsorption onto the coal surface; thus, it is the pore surface area of the coal that determines the maximum gas holding potential of a reservoir [2]. As a natural porous media, coal usually has an incredibly complex pore structure, including many micropores, cleats, and fissures, and the specific surface area of coal generally reaches 6~15 m^2/g [3–6]. As a result, coal shows a strong adsorption capacity to some gases and the adsorption gas accounts for more than 90% of the gas storage within the coal [7]. Coal exhibits different adsorption capacities for different gases. Many scholars have reported that the carbon dioxide sorption capacity of coal is larger than that of methane and nitrogen [8–11]. Adsorption tests on coal from

the Yangquan coal mine showed that the sorption capacity ratio of CO₂, CH₄, and N₂ was about 6.0:2.3:1 [12] and the capacity ratio for an Akabira coal sample was 5.5:2:1 [13]. The study showed that the adsorption capacity ratio of carbon dioxide and methane varied from 2:1 to 4:1 [14]. Hence, it is very useful to study the gas adsorption characteristics of a coal body in order to estimate coalbed methane reserves and their recoverability.

During the first half of the last century, several adsorption models were developed, these being the Langmuir equation, the extended Langmuir equation, the Brunauer–Emmet–Teller (BET) equation, the Dubinin–Astakhov (D-A) equation and the Dubinin–Radushkevich (D-R) equation, which were proposed successively [14–16]. According to the trend of increasing sorption capacity with the increasing pressure, the solid gas isotherm sorption curves generally are divided into six categories [17,18]. Coal gas adsorption belongs to the physical adsorption category, and its isothermal sorption curves are mainly in category I and category II [19,20]. Some studies have shown that the Langmuir equation could be used to describe the coal gas isotherm sorption with satisfactory precision [21–25]. However, it is doubtful that monolayer adsorption can describe adsorption in a complex pore structure because the Langmuir equation is deemed to be applicable to gas molecular adsorption on an open surface. From the study of methane adsorption on crushed organic shale and coal, a dual-site adsorption model was used to describe the gas sorption in coal and shale [26]. Based on the measured adsorption data analysis, it was concluded that the fitting precision of the Toth equation was superior to that of the Langmuir equation [27]. The study of gas adsorption in coal indicates that the Langmuir equation, the BET equation, and the D-R equation can each properly describe the coal methane isotherm adsorption. However, for the isothermal adsorption of carbon dioxide, only the D-R equation reaches the appropriate fitting precision [14]. According to the study of supercritical gas adsorption on coal, it was found that the D-R equation also can describe the isothermal adsorption curve of supercritical carbon dioxide [28]. From the adsorption capacity study of organic-rich marine shale samples, the D-R equation showed high fitting accuracy, the Langmuir equation could meet the evaluation of adsorption capacity, and the BET equation had the worst fitting effect [24,29]. The D-R equation also had a satisfactory precision in describing the isothermal adsorption of supercritical carbon dioxide of differently ranked coals [30].

Nevertheless, while previous studies have provided useful insights into the experimental investigation and modeling of gas sorption, few studies have been conducted on the comparative analysis of the adsorption models of bituminous coal. Thus, it is necessary to understand better the effectiveness of the adsorption models for different gases. The bituminous coal of Xutuan Coal Mine in Anhui of China was taken as the research subject for this investigation. In a previous study, a series of gas adsorption tests on coal from the main coal seam had been carried out with a bespoke Gas Adsorption and Strain Testing Apparatus (GASTA). All tests were performed at 303 K (30 °C) on dry pulverized coal samples (0.18–0.25 μm). The gas sorption capacity of methane, carbon dioxide and nitrogen was measured, the two-parameter Langmuir equation, BET equation, and D-R equation were used to describe the isothermal sorption curves, and the fit precision was analyzed. Finally, a comparative analysis of the effectiveness of the three models in modeling adsorption of the different gases was carried out.

2. Methodology

2.1. Background

The Xutuan Coal Mine is located in Mengcheng County, southwest of Suzhou City, in the Anhui province of China, and belongs to the Huabei coalfield, as shown in Figure 1. The Xutuan coalfield belongs to the Permian coal system. The mine is classified as a high gas mine (the relative gas emission is 22 m³/t). The main coal seam of the mine is Coal Seam 32. The coal samples SA3 and SA8 were derived from Coal Seam 32. Samples with a particle size range of 0.25 mm to 0.18 mm were prepared in accordance with GB/T 474 and the coal samples were entirely dried under anaerobic conditions. The coal petrology parameters of the coal samples are listed in the following Tables 1 and 2.

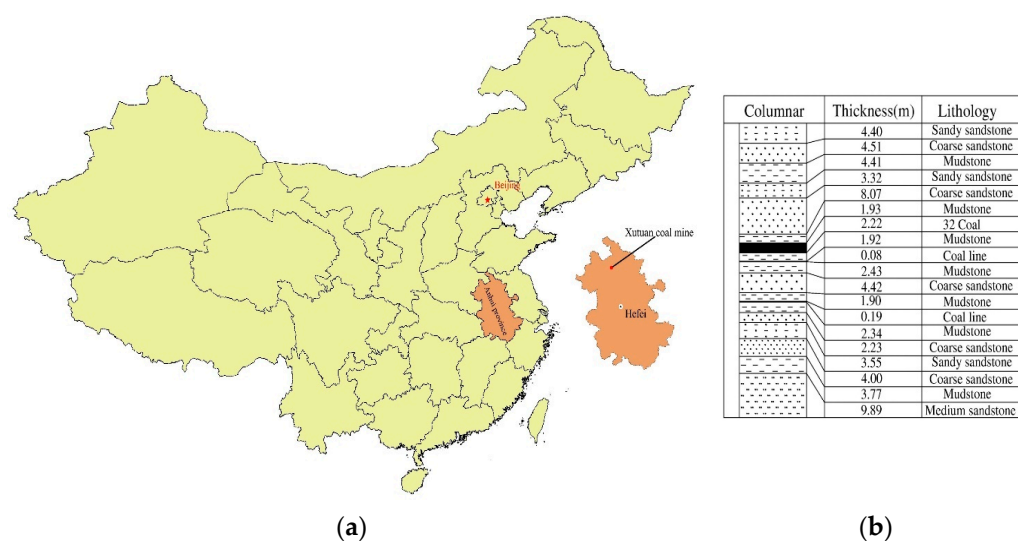


Figure 1. (a) The location of Xutuan Coal Mine in China. (b) The borehole diagram of Coal Seam 32.

Table 1. Maceral statistics of sampling coal samples.

Coal Sample	Organic Component (%)				Inorganic Component (%)	R_{max} (%)
	Vitrinite	Semi-Vitrinite	Inertinite	Exinite		
SA3	66.93	9.68	14.53	8.86	7.11	0.82
SA8	72.96	9.79	12.06	5.19	7.55	0.95

Table 2. The proximate analyses of sampling coal samples.

Coal Sample	Mad (%)	Aad (%)	St.d (%)	P.d (%)	Vdaf (%)
SA3	1.51	18.85	0.68	0.0089	35.39
SA8	1.41	17.88	0.53	0.0112	31.93

"Mad" is the moisture content; "Aad" is the ash content, air-drying basis; "St.d" is the sulfur content; "P.d" is the phosphorus content; "Vdaf" is the volatile matter, dry ash-free basis.

2.2. Experimental Apparatus

The gas adsorption measurement was carried out using the GASTA. The adsorptive capacity of coal samples was calculated by a volumetric method. Inert gas was used to calibrate the free space volume of the sample chamber. The measured pressure in the chambers was then used to calculate the adsorption capacity through the real gas state equation.

The main parameters of the GASTA are described as follows:

- (1) The pressure range of the reference chamber and the sample chamber: 0–20 MPa;
- (2) Reference chamber and the sample chamber size: inner diameter 60 mm, inner height 80 mm;
- (3) Pressure sensors measurement range: 0–25 MPa, 0.25%;
- (4) Constant temperature control range: room temperature–100 °C ± 0.1 °C.

All experiments were performed at 303 K (30 °C) on dry pulverized coal samples (0.18–0.25 µm).

The reference chamber, the sample chamber and their auxiliary pressure transducers are the core components of the test apparatus. The components of the apparatus are shown in Figures 2 and 3.

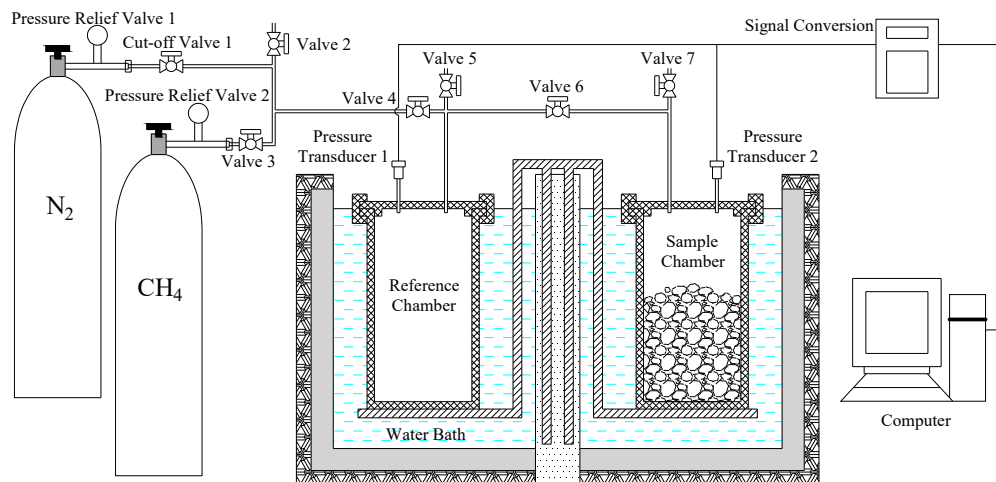


Figure 2. The schematic diagram of the GASTA.

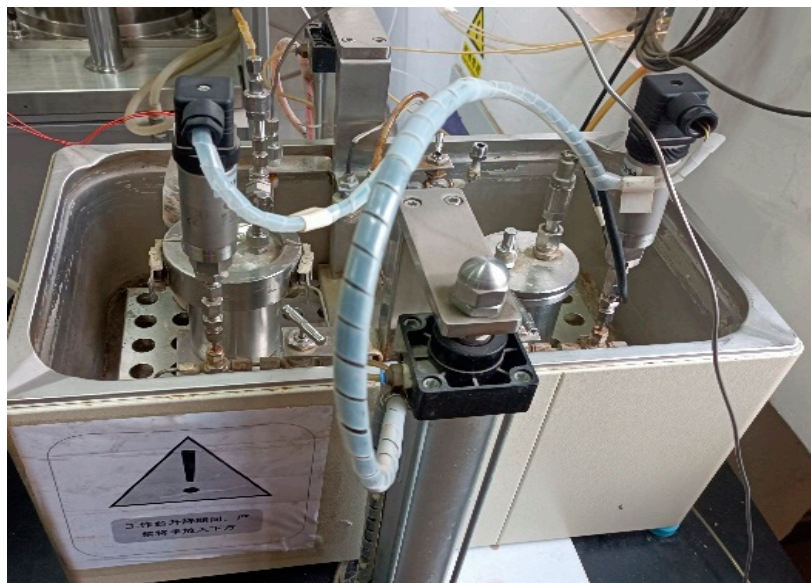


Figure 3. Physical experimental setup of GASTA2.3. Measurement and calculation method of adsorption capacity.

In this paper, the adsorption capacity was calculated by using the volumetric method. The pressure of the sample chamber and the reference chamber was measured by the pressure transducers. The adsorption capacity then was calculated using the real gas state equation. Hence, the adsorption capacity refers to the excess (or Gibbs) adsorption capacity.

The ideal gas state equation is a gas state equation that describes the relationship between the pressure, volume, mass, and temperature. The real gas state is biased from the ideal gas state under different conditions. Thus, different real gas state equations are established. In this study, the gas state Soave–Redlich–Kwong (SRK) equation was used to calculate the amount of the gas in the fixed volume under a certain pressure. The SRK equation is shown as follows:

$$p = \frac{RT}{V_m - b} - \frac{\alpha a}{V_m(V_m + b)} \quad (1)$$

where

$$\alpha = [1 + (0.48508 + 1.55171\omega - 0.15613\omega^2)(1 - \sqrt{T/T_c})]^2 \quad (2)$$

$$a = \frac{0.42747 R^2 T_c^2}{P_c} \quad (3)$$

$$b = \frac{0.08664 R T_c}{P_c} \quad (4)$$

and p is the gas pressure, MPa; R is the gas constant, $8.314 \text{ J}\cdot\text{mol}^{-1}\cdot\text{K}^{-1}$; T is the thermodynamic temperature, K; V_m is the molar volume, $\text{mL}\cdot\text{mol}^{-1}$; T_c is the gas critical temperature, K; P_c is the gas critical pressure, MPa; and ω is the gas acentric factor, related to the polarity of a gas molecule.

The parameters of T_c , P_c , ω are related only to the gas molecules. The gas pressure p and the thermodynamic temperature T are measured by the attached sensor. The molar volume V_m is calculated by the single variable solution of Excel using the SRK equation.

The experimental steps are as follows:

- (1) Experimental preparation. First the water bath controller is opened and the adsorption reaction temperature set. The size and weight of the coal sample are then measured and the coal sample is loaded into the sample chamber. Finally, the test system is tested for withstand voltage to ensure the tightness of the chamber test system.
- (2) The determination of free space volume. For the gas sorption experiments, the inert gas helium, which is not absorbed by coal, is injected into the reference chamber. The injected helium amount is calculated from the calibration volume of the reference chamber and measured pressure through the SRK equation. The valve between the reference chamber and sample chamber is then opened. After the gas pressure of the reference chamber and the sample chamber reaches equilibrium, the free volume of the sample chamber can be calculated from the injected helium amount and the equilibrium pressure.
- (3) Determination of gas adsorption capacity. The same steps then were carried out for methane, carbon dioxide, and nitrogen and the adsorption capacity calculated using the SRK equation, with the fixed sample chamber free volume and measured pressures.

3. Gas Isotherm Sorption Analyses

3.1. Coal Sorption Capacity Analyses

The main coal seam gas (nitrogen, methane, and carbon dioxide) sorption experiments on coal samples SA3 and SA8 were carried out. A sorption time of 12 h at equilibrium pressure was utilized. A group of sorption experiments generally had seven adsorption sites and seven desorption sites. So, a group of sorption experiments usually would take a week to complete. In this investigation, the adsorption capacity of three different gases to two coal samples was tested, and six groups of sorption experiments were carried out. The sorption isotherm curves of the coal samples are shown in Figure 4.

As shown in Figure 4, under the same equilibrium pressure, the sorption capacity ranking order of the bituminous coal to the three different kinds of gases was $\text{CO}_2 > \text{CH}_4 > \text{N}_2$. This sorption capacity order has been verified by most scholars [13,14,31]. The sorption capacity ratio of Xutuan Coal Mine's Coal Seam 32 to carbon dioxide, methane and nitrogen was about 6.0:2.3:1. The sorption experiment of the Nantong coal sample indicated the ratio of the three gases was 6.9:2.8:1; that of the Yangquan coal sample was 4.6:3.2:1; that of the Tiffany coal sample was 6.7:3.5:1 [31]; that of the Akabira coal sample was 5.5:2:1 [13]; and the study of Harpalani et al., showed the adsorption capacity ratio of carbon dioxide and methane was from 2:1 to 4:1 [14]. Some scholars have proposed that the adsorption capacity of coal to a gas is related to the boiling point of the gas. The higher the boiling point of the gas, the deeper the adsorption potential, the lower the diffusion rate, and the larger the adsorption capacity of coal to the gas. The order of the boiling points of the three gases is $\text{CO}_2 > \text{CH}_4 > \text{N}_2$. So, under the same equilibrium pressure, the adsorption capacity of CO_2 is the largest, and N_2 is the least [8].

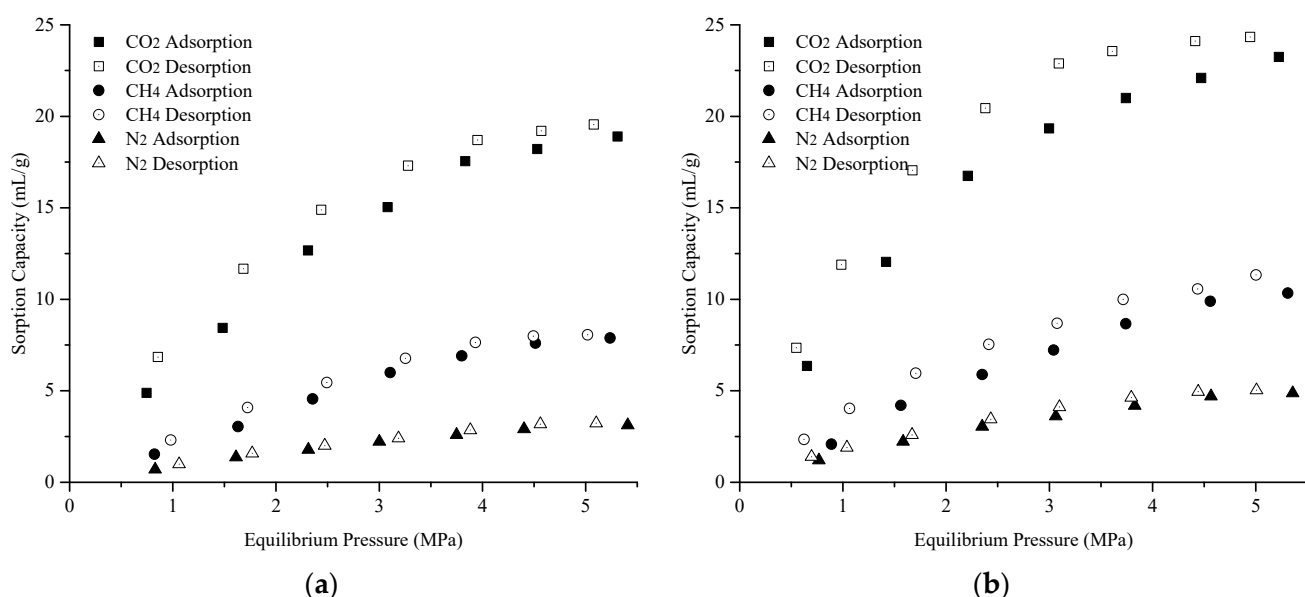


Figure 4. The sorption capacity under different equilibrium pressures for different gases: (a) Coal sample SA3; and (b) coal sample SA8.

As shown in Figure 4, the adsorption isotherm curve is not the same as the desorption curve. The desorption curve always lags behind the adsorption curve. Actually, the desorption hysteresis phenomenon widely exists in coals to different metamorphic degrees [14,32,33], and the desorption hysteresis effect of dry coal samples is more evident than for other coal samples. In practice, during the adsorption process, the coal matrix expands; and with the desorption process the coal matrix shrinks [14,22,34]. The plasticity of the coal matrix determines the hysteresis of expansion after shrinkage, so at the same equilibrium pressure, the adsorption capacity in the desorption process is larger than that in the adsorption process. Because the adsorption curve and desorption curve are not identical, the desorption curve is more appropriate when evaluating of the CBM reserves.

For any specific gas, the adsorption capacity of coal sample SA8 was larger than that of coal sample SA3. It is generally believed that the factors affecting the adsorption amount of coal are the water content, the vitrinite content, and metamorphic degree. Some scholars have established that there is a positive correlation between the coal gas adsorption capacity and the vitrinite content [27,32]. Chaback et al. tested the isothermal adsorption behavior of five differently ranked coal samples and demonstrated that the influence of coal rank on adsorption capacity did not show a clear and consistent correlation [32]. Other researchers have suggested that coal gas adsorption capacity is related to the water content of the coal [8,35]. Based on test results from the present investigation and on the results of previous research investigations, the effect of coal quality on gas adsorption is probably related to different components of the coal. Therefore, it is difficult to reach consistent conclusions about the effect of coal quality and coal rank on the adsorption capacity.

3.2. The Fitting Analysis of Adsorption Model

3.2.1. Introduction of Two-Parameter Adsorption Models

Based on the hypothesis of surface adsorption sites, Langmuir derived the most popular solid-gas two-phase adsorption model [15]. The Langmuir adsorption isotherm equation of usually is expressed by the following Formula (5):

$$\frac{V}{V_L} = \frac{P}{P + P_L} \quad (5)$$

where V (mL) is the adsorbed volume at equilibrium pressure P (MPa); V_L is the maximum monolayer capacity, also known as the Langmuir volume, mL; P_L is the Langmuir pressure, MPa; it refers to the pressure when the sorbed volume is half of the Langmuir volume $V_L/2$.

According to the BET theory, the physical adsorption of solid to gas is the result of van der Waals forces. The van der Waals force exists not only amongst the gas molecules but also between the pore walls and gas molecules. Hence, solid–gas adsorption can form a multimolecular layer. The adsorption energy of solid to gas forms the first molecular layer and the adsorption energy of gas to gas forms the second and the additional adsorbed molecular layers. The BET model can describe different types of adsorption isotherm curves [14,16].

The BET theory also is a surface adsorption model, but it is a multi-molecular layer adsorption model. The following Formula (6) is generally used to describe the adsorption isotherm of solid to gas.

$$\frac{1}{V(P_0/P - 1)} = \frac{1}{V_m C} + \frac{C - 1}{V_m C} \frac{P}{P_0} \quad (6)$$

where V_m is the monolayer volume, mL; C is a constant; P_0 is the saturation vapor pressure, MPa. The larger the value of C , the earlier that the multilayer formation will occur.

Based on the Polanyi adsorption theory, Dubinin proposed the Theory of Volume Filling of Micropores (TVFM) to explain the adsorption phenomena in porous media. Dubinin and Astakhov proposed an equation representing the isotherms that obeyed TVFM. Known as the Dubinin–Astakhov (D-A) equation, it is expressed as Formula (7):

$$V = V_0 \exp[-D \{\ln(\frac{P_0}{P})\}^n] \quad (7)$$

where V is the amount adsorbed, mL; V_0 is the volume of micropores, mL; n is the structural heterogeneity parameter, a small number varying between 1 and 4; and D is a constant for a particular adsorbent–adsorbate system [14].

Dubinin and Radushkevich suggested that the value of $n = 2$ may be appropriate for some cases, and the equation (D-R equation) can be modified as Formula (8):

$$V = V_0 \exp[-D \{\ln(\frac{P_0}{P})\}^2] \quad (8)$$

The above equation is called the Dubinin–Radushkevich (D-R) equation.

3.2.2. Comparison and Analysis of the Fitting Results for Different Adsorption Models

The Langmuir equation, BET equation, and D-R equation were imported into the data analysis software Origin as custom functions, and then Origin was used to fit and analyze the experimental data to obtain each parameter of the fitted equations, as shown in Table 3.

Table 3. The critical parameters of CO₂, CH₄ and N₂.

Physical and Chemical Parameters	CO ₂	CH ₄	N ₂
T_c (°C)	31.05	-82.55	-146.95
P_c (MPa)	7.375	4.60	3.39
ω	0.250	0.008	0.040
Ionization potential (eV)	15.6	13.79	13.0
Boiling point (°C)	-56.55	-161.5	-195.8
Diameter (nm)	0.456	0.414	0.374

In the present investigation, two parameters of the Langmuir equation, the BET equation, and D-R equation were used to fit and analyze the adsorption and desorption data. The above three models were imported into the data analysis software ‘Origin’ by

a user-defined function. Then, Origin was used to fit and analyze the test data and the parameters of the fitting equation were obtained.

The Langmuir equation, the BET equation, and the D-R equation all involve two fitting parameters, but the BET equation and the D-R equation also involve the saturated vapor pressure of the adsorbed gas. In the present study, the adsorption experiments were carried out with a water bath temperature of 30 °C. At this temperature, the saturated vapor pressure of CO₂ was 7.21 MPa. However, the temperature of 30 °C was higher than the critical temperature of CH₄ and N₂. This means that at this temperature, CH₄ and N₂ do not exert a saturated vapor pressure. A formula for calculating the pseudo saturated vapor pressure of a gas by using the contrasting temperature to modify the critical pressure has been proposed as Equation (9) [36]:

$$P_0 = P_C (T/T_C)^2 \quad (9)$$

where P_0 is the pseudo saturated vapor pressure, MPa; P_C is the critical pressure of the gas, MPa; T is the gas temperature, K; and T_C is the critical temperature of the gas, K.

With Equation (9) and the critical parameters, the pseudo saturated vapor pressure of CH₄ and N₂ at 30 °C were 11.64 MPa and 19.56 MPa. Hence, when the BET equation and D-R equation are used to predict the gas adsorption capacity, the saturated vapor pressure of CO₂ is 7.21 MPa, and CH₄ and N₂ are 11.64 MPa and 19.56 MPa, respectively.

(1) Fitting analysis of the Langmuir equation

The test data of coal samples SA3 and SA8 were fitted by the Langmuir equation, as shown in Figures 5 and 6, respectively. The fitting parameters of coal sample SA3 and SA8 by the Langmuir equation are shown in Tables 4 and 5.

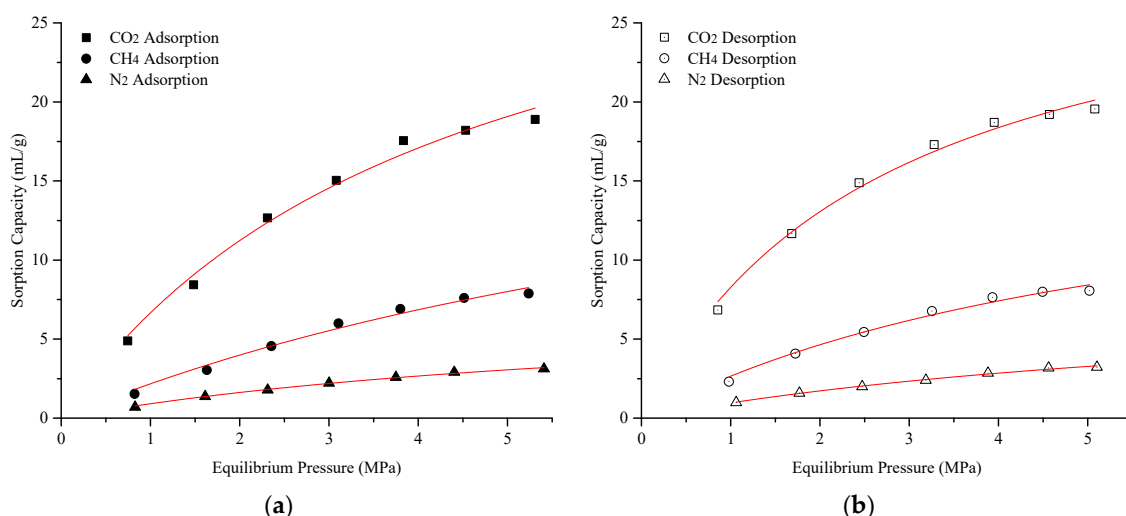


Figure 5. The test data of coal samples SA3: (a) before fitted by the Langmuir equation; and (b) after fitted by the Langmuir equation.

Table 4. The Langmuir fitting parameters of coal sample SA3.

Test-Path	V_L (cm ³ /g)	P_L (MPa)	Correlation Coefficient R^2
CO ₂ Adsorption	35.72	4.36	0.989
CH ₄ Adsorption	24.39	10.22	0.985
N ₂ Adsorption	7.41	7.12	0.996
CO ₂ Desorption	30.99	2.75	0.992
CH ₄ Desorption	18.41	5.93	0.986
N ₂ Desorption	8.13	7.43	0.995

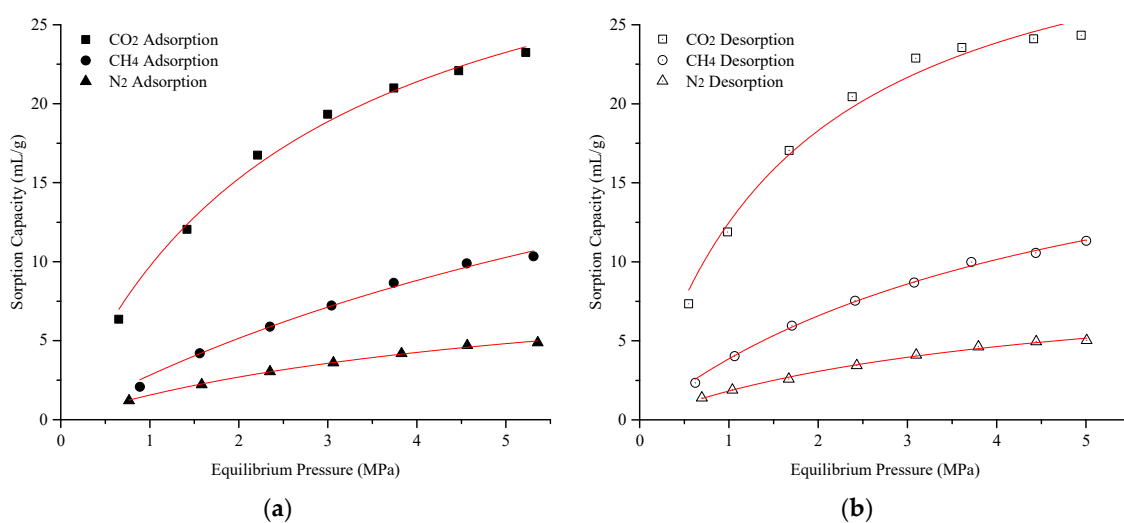


Figure 6. The test data of coal samples SA8: (a) before fitted by the Langmuir equation; and (b) after fitted by the Langmuir equation.

Table 5. The Langmuir fitting parameters of coal sample SA8.

Test-Path	V _L (cm ³ /g)	P _L (MPa)	Correlation Coefficient R ²
CO ₂ Adsorption	35.72	2.68	0.994
CH ₄ Adsorption	30.44	9.82	0.992
N ₂ Adsorption	10.09	5.48	0.997
CO ₂ Desorption	34.25	1.74	0.986
CH ₄ Desorption	22.13	4.72	0.999
N ₂ Desorption	9.51	4.20	0.996

From the comparison between the test data shown above and the fitting lines of the Langmuir equation in Figures 5 and 6, it was observed that the Langmuir equation can describe the isothermal sorption of CO₂, CH₄, and N₂ accurately. From the correlation coefficient of the data in Tables 4 and 5, the correlation coefficient of the Langmuir equation to the three kinds of gases all were higher than 0.985, which means that the sorption capacity prediction of the Langmuir equation achieved satisfactory results, and the Langmuir equation has significant capability in the guidance of gas reserves evaluation.

The Langmuir adsorption model assumes that the adsorption sites on the surface of the adsorbent are one-to-one corresponding to the adsorbate molecules. When the adsorption sites of all adsorbents are occupied by gas molecules, the maximum adsorption capacity of the adsorbent is reached, i.e., the Langmuir volume. According to the fitting data in Tables 4 and 5, coal has a different maximum adsorption capacity for different gases. For different gases, the total number of adsorption sites on coal surfaces is different. Coal has the most adsorption sites for carbon dioxide, followed by methane and nitrogen. The Langmuir volume and the Langmuir pressure in the desorption process are less than that of the adsorption process. This phenomenon also illustrates the desorption hysteresis effect. The gas drainage process corresponds to the process of gas desorption. Therefore, it is more accurate to use desorption fitting data to evaluate the gas storage stock.

(2) Fitting analysis of the BET equation

The test data of coal samples SA3 and SA8 were fitted by the BET equation, as shown in Figures 7 and 8, respectively. The fitting parameters of coal sample SA3 and SA8 by the BET equation are shown in Tables 6 and 7.

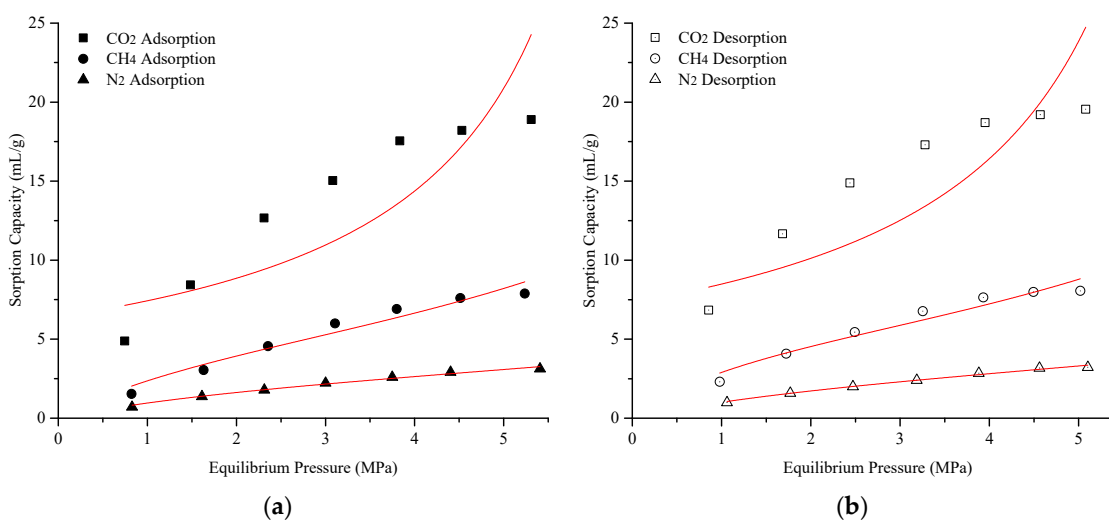


Figure 7. The test data of coal samples SA3: (a) before fitted by the BET equation; and (b) after fitted by the BET equation.

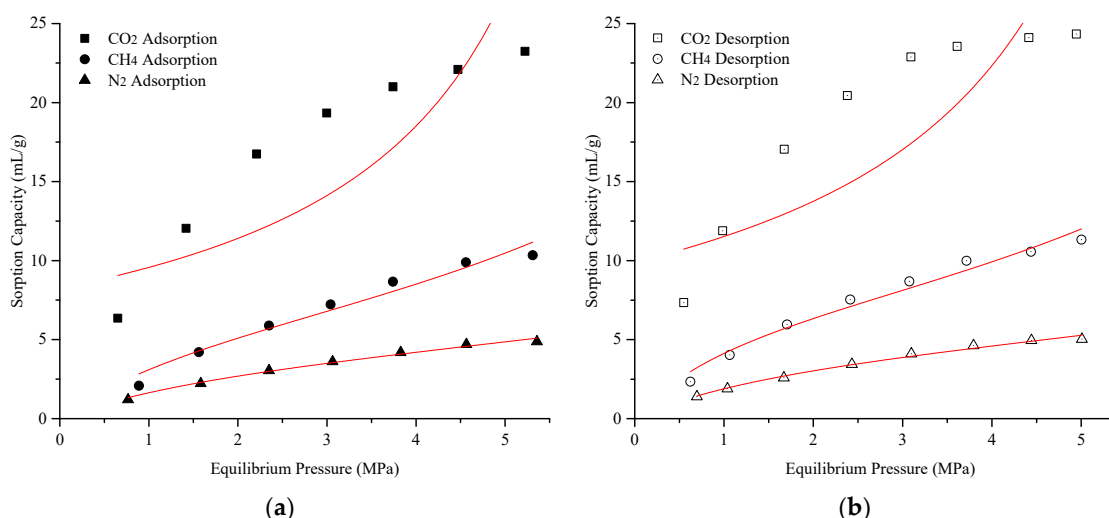


Figure 8. The test data of coal samples SA8: (a) before fitted by the BET equation; and (b) after fitted by the BET equation.

Table 6. The BET fitting parameters of coal sample SA3.

Test-Path	V _m (cm ³ /g)	C (MPa)	Correlation Coefficient R ²
CO ₂ Adsorption			0.555
CH ₄ Adsorption	5.62	6.63	0.954
N ₂ Adsorption	3.20	7.34	0.988
CO ₂ Desorption			0.474
CH ₄ Desorption	5.74	9.10	0.948
N ₂ Desorption	3.48	7.05	0.991

Table 7. The BET fitting parameters of coal sample SA8.

Test-Path	V _m (cm ³ /g)	C (MPa)	Correlation Coefficient R ²
CO ₂ Adsorption			0.459
CH ₄ Adsorption	7.10	7.04	0.965
N ₂ Adsorption	4.80	8.86	0.991
CO ₂ Desorption			0.437
CH ₄ Desorption	7.75	10.12	0.976
N ₂ Desorption	5.04	10.25	0.989

It can be seen from Figures 7 and 8 that it is difficult to fit the BET equation to the sorption isotherm curve of carbon dioxide, but it has a preferable fitting effect on methane and nitrogen. From the data summarized in Tables 6 and 7, the correlation coefficient of the BET equation to CO₂ absorption was about 0.5, but the correlation coefficient of the BET equation to CH₄ and N₂ absorption was greater than 0.95. Compared with the Langmuir equation, the BET equation had a poor fitting correlation with the adsorption isothermal curve of coal gas. The BET adsorption model is a multi-layer molecular adsorption model and the parameter V_m is the monolayer adsorption capacity. According to the fitting data, the monolayer adsorption capacity of a coal for methane is higher than that for nitrogen.

(3) Fitting analysis of the D-R equation

The physical test data of coal samples SA3 and SA8 were fitted by the D-R equation, as shown in Figures 9 and 10, respectively. The fitting parameters of coal sample SA3 and SA8 by the D-R equation are shown in Tables 8 and 9.

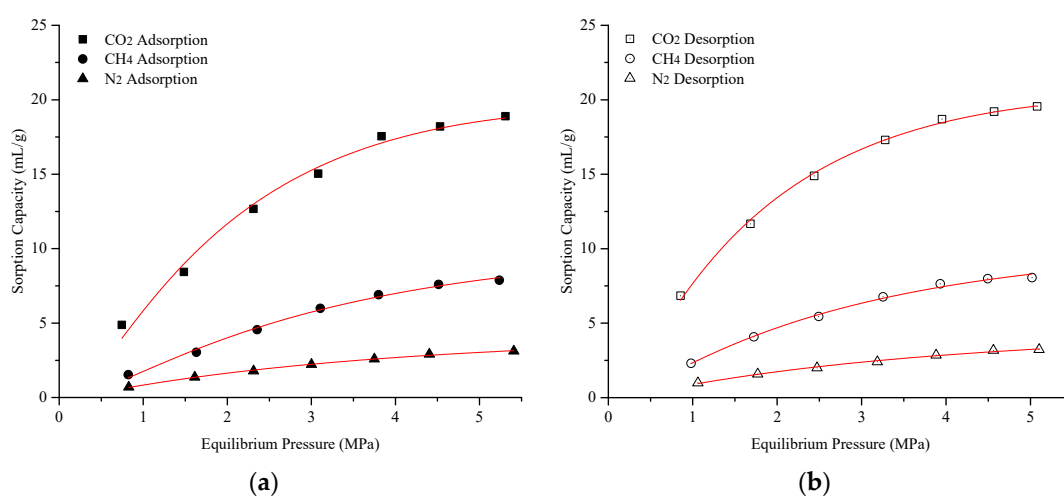


Figure 9. The test data of coal samples SA3: (a) before fitted by the D-R equation; and (b) after fitted by the D-R equation.

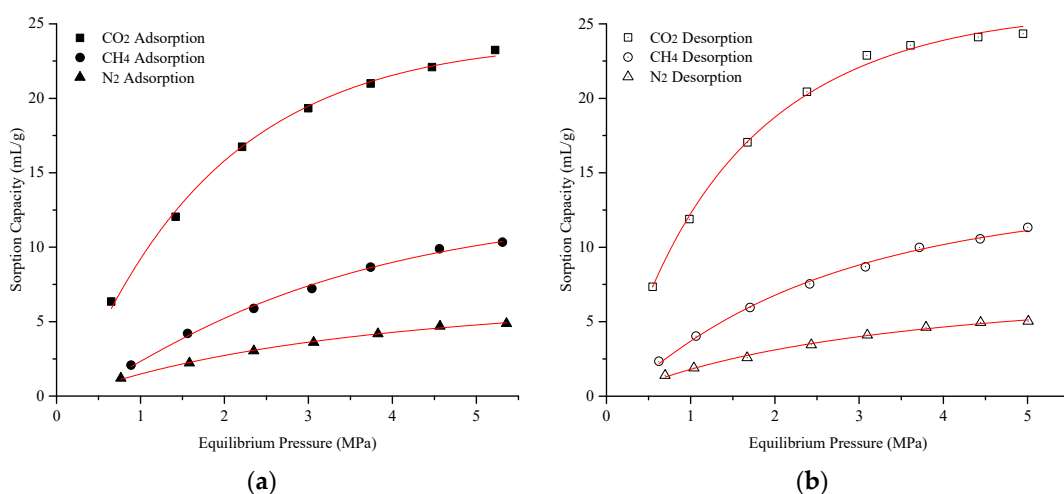


Figure 10. The test data of coal samples SA8: (a) before fitted by the D-R equation; and (b) after fitted by the D-R equation.

Table 8. The D-R fitting parameters of coal sample SA3.

Test-Path	V_0 (cm ³ /g)	D (MPa)	Correlation Coefficient R ²
CO ₂ Adsorption	19.32	0.31	0.990
CH ₄ Adsorption	9.65	0.28	0.995
N ₂ Adsorption	4.27	0.18	0.998
CO ₂ Desorption	20.19	0.24	0.998
CH ₄ Desorption	9.82	0.24	0.995
N ₂ Desorption	4.57	0.19	0.994

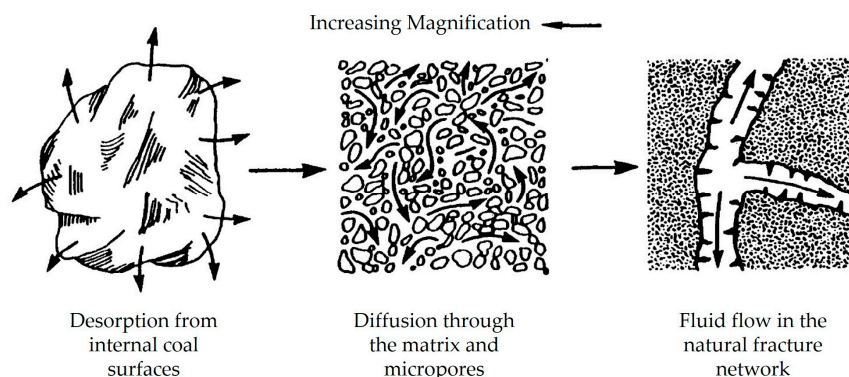
Table 9. The D-R fitting parameters of coal sample SA8.

Test-Path	V_0 (cm ³ /g)	D (MPa)	Correlation Coefficient R ²
CO ₂ Adsorption	23.41	0.24	0.997
CH ₄ Adsorption	12.31	0.28	0.996
N ₂ Adsorption	6.53	0.17	0.997
CO ₂ Desorption	25.50	0.19	0.997
CH ₄ Desorption	12.90	0.21	0.997
N ₂ Desorption	6.77	0.15	0.995

In Figures 9 and 10, the D-R equation exhibits excellent fitting results for the sorption of the three gases. According to the data in Tables 8 and 9; the correlation coefficient of the D-R equation to the different gases is higher than 0.99, which is more accurate than the Langmuir equation. For the D-R model of micropore filling theory, it is assumed that microporous molecular-scale porous media are present, due to the proximity between the hole wall and superposition of the adsorption potential. This effect makes the gas adsorption mechanism in porous media entirely different from that at an open surface. The adsorption behavior of gas in micropores is pore filling, not the surface coverage mechanism described by the theory of Langmuir, and BET. For the different gases, coals show different molecular scales of filled micropore volume V_0 . From the above fitting data, it can be seen that the order of filled micropore volume for the three kinds of gas is $V_0(\text{CO}_2) > V_0(\text{CH}_4) > V_0(\text{N}_2)$.

4. Experimental Analysis of Gas Permeability Characteristics

Once the pressure in the coal seam is reduced, coal becomes less capable of retaining coal seam gas molecules in adsorbed form. The gas molecules start detaching themselves from the surface of the pores and microfractures and the process of desorption is initiated, making more gas available for flow towards the gas drainage well [37]. The rate of flow is primarily dependent on the diffusion characteristics and the permeability of coal. Figure 11 shows the three distinct processes involved in the transport of CSG, starting with desorption from the internal coal surfaces, then diffusion through the matrix and micropores towards the cleats/fractures, and finally, the Darcy flow of gas in the natural fracture network.

**Figure 11.** Transport of coal seam gas in coal [37].

Thus, the gas sorption and permeability characteristics of a coal provide an essential basis for the evaluation of coalbed methane reserves and their recoverability. Coal sorption characteristics not only determine the coal sorption capacity, but also have apparent influence on coal permeability. The permeability of the same coal sample to N₂, CH₄, and CO₂ gases was tested under the standard triaxial testing method. The permeability test of variable inlet pressure was carried out under the conditions of constant confining pressure (confining pressure = axial pressure) with carbon dioxide, methane, and nitrogen as seepage gas, respectively.

4.1. Experimental Design and Procedures

The experimental system was designed for the determination of coal sample permeability using Darcy's law, and the amount of replacing gas and the amount of replaced gas was determined by flow meter and exhausted gas analysis. The main parameters of the experimental system are as follows: the maximum loading pressure of the coal core is 100 KN; the design pressure of the autoclave is 20 MPa; the diameter of the autoclave is 150 mm and the height is 150 mm; flow meter range of 0 to 15 slm; the range of the pressure sensor is 0–25 MPa; the temperature test range is 15–100 °C with the error of ±0.1 °C; the total power of the equipment is 3.5 KW. The experimental test principle and experimental equipment are shown in Figure 12. The experimental system is mainly composed of the following subsystems: loading system; autoclave system; gas supply and decompression system; temperature simulation system; acquisition and control system; strain testing system; and related auxiliary facilities.

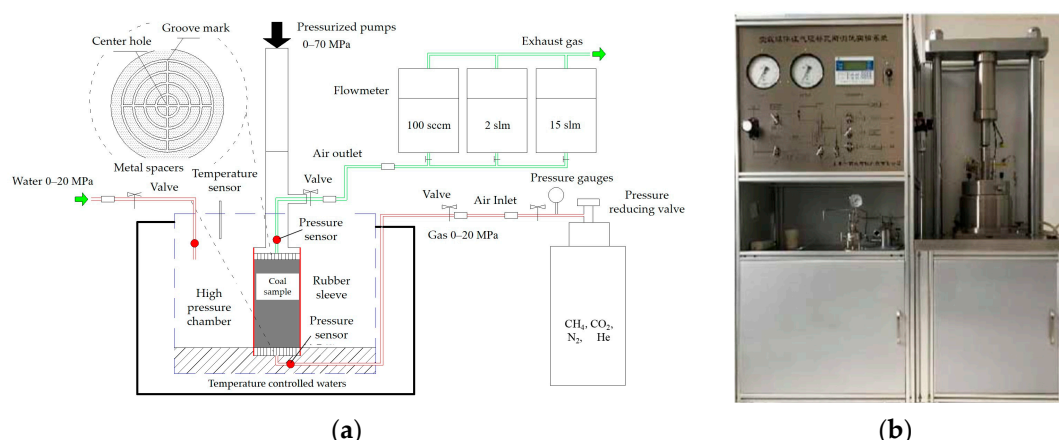


Figure 12. The experimental test principle and experimental equipment: (a) Experimental procedure; and (b) experimental equipment.

In this article, it is assumed that the pore pressure during gas percolation in the coal sample is gradually decreasing, which indicates that the average of the percolation inlet pressure and outlet pressure can represent the average pore pressure. The seepage inlet pressure can be changed by adjusting the pressure reducing valve to obtain different average pore pressures. Pressure sensors are installed at both the inlet and outlet of the seepage stream, and in combination with an outlet flow meter, the permeability at the average pore pressure can be obtained. The pore pressure inside the coal sample is changed by adjusting the gas pressure at the inlet end, and different ground stresses are simulated by the change in radial pressure. It is generally considered that the ground stress is hydrostatic pressure, so this experiment keeps the radial pressure and axial pressure in the equal state in each step of the circumferential pressure loading, i.e., the coal sample is in the three-way isobaric pressure state. The design pressure values of the inlet pore pressure are shown in Table 10.

Table 10. Design pressure values of inlet pore pressure.

Circumferential Pressure/MPa	Inlet Pore Pressure/MPa
2	0.50, 0.75, 1.00, 1.25, 1.50, 1.75
3	0.50, 0.75, 1.00, 1.25, 1.50, 1.75, 2.00, 2.25, 2.50, 2.75
5	0.50, 1.00, 1.50, 2.00, 2.50, 3.00, 3.50, 4.00, 4.50
6	0.50, 1.00, 1.50, 2.00, 2.50, 3.00, 3.50, 4.00, 4.50, 5.00, 5.50

4.2. Analysis of Experimental Results

In this study, percolation experiments were conducted for coal sample SA3 and coal sample SA8, but the differences in permeability characteristics between the two coal samples were not obvious, so only the results of percolation experiments for coal sample SA3 is analyzed in the experimental results presented below. In most cases, the measured permeability of the three gases was similar to a high degree, i.e., the coal samples did not show significant differences in the permeability characteristics for different gases. However, at higher pore pressures, the permeability of coal samples to CO₂ differs from that of CH₄ and N₂. Therefore, in the following, when analyzing the permeability characteristics of different pore pressures, only the experimental results of the permeability of methane are listed when the permeability characteristics of the three gases are basically the same. The result shows that the permeability of CO₂ was found to be lower than that of the other coal seam gas constituents, CH₄ and N₂, due to their different sorption characteristics, as shown in Figure 13. When nitrogen (N₂), methane (CH₄), and carbon dioxide (CO₂), which are usually present in coal seam gases, were used separately as gas environments in the seepage tests, the respective permeability curves exhibited no significant difference and yielded similar seepage characteristics. However, under constant confining pressure, the permeability of coal samples to carbon dioxide was shown to be different from that of the other two gases, which is depicted in Figure 13.

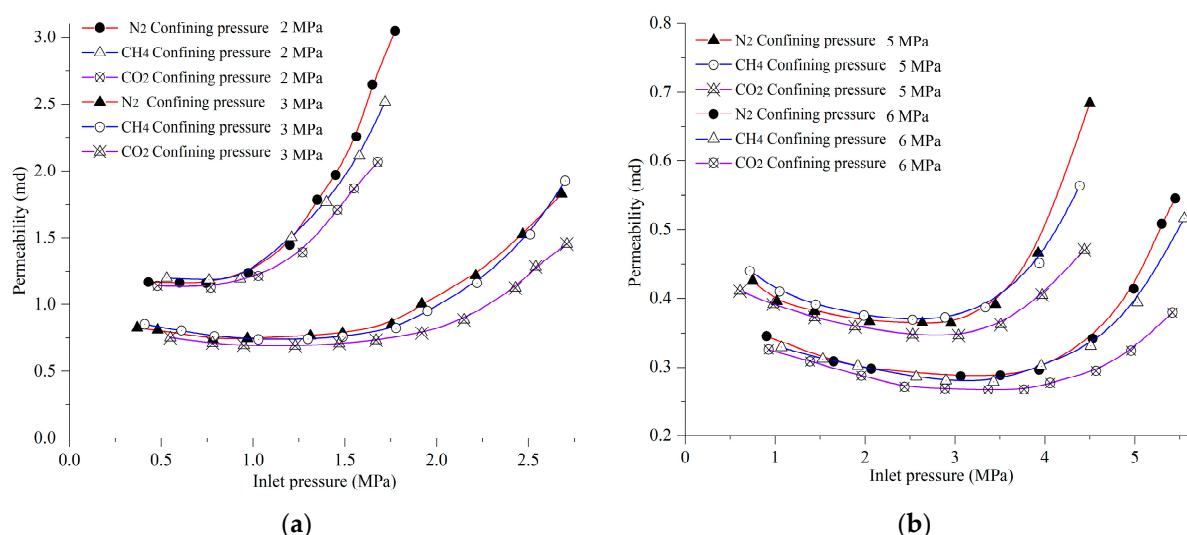


Figure 13. Test results on N₂, CH₄ and CO₂ seepage in coal samples: (a) Under 2 MPa/3 MPa constant confining pressure; and (b) under 5 MPa/6 MPa constant confining pressure.

It can also be observed in Figure 13 that the permeability curves of nitrogen and methane are nearly identical. On the other hand, that of carbon dioxide is generally lower than the first two curves, and the difference becomes more evident with an increase in the pore pressure. Since the molecular diameters of the three gases (0.364 nm for N₂, 0.380 nm for CH₄, and 0.330 nm for CO₂) are quite close, this influencing factor of the gas slippage

effect does not explain the difference between the three gas permeability curves. The main sources of this difference are seemingly the adsorption and expansion effects of the coal matrix. In contrast to nitrogen and methane, carbon dioxide possesses a stronger adsorption capacity in coal samples. With an increase in gas pressure, the expansion deformation of the coal matrix is more pronounced, which is equivalent to exerting an action on the cracks expanded by the gas extrusion. Therefore, when the inlet pressure is high, the nitrogen permeability is the highest, that of methane is the medium, and that of carbon dioxide is the lowest.

5. Conclusions

The study of gas sorption characteristics using physical testing helps not only to explain the mechanism of gas extraction but also provides an essential basis for the evaluation of coalbed methane reserves and recoverability. The bituminous coal of the Xutuan Coal Mine in the Huabei coalfield in China was taken as the research subject in the present study. A series of gas adsorption tests were carried out, using the bespoke Gas Adsorption and Strain Testing Apparatus (GASTA). The main conclusions were as follows:

- (1) The gas adsorption capacity of the coal seam was measured with the GASTA instrumentation. The isothermal sorption curves of the bituminous coal samples to CO₂, CH₄, and N₂ were plotted. It was observed that the isothermal sorption curves of the three gases indicated that the sorption capacity of CH₄ was larger than that of N₂ but was less than for CO₂. Furthermore, the sorption capacity ratio of the Xutuan Coal Mine Coal Seam 32 material to CO₂, CH₄, and N₂ was about 6.0:2.3:1.
- (2) The adsorption capacity of the coal samples in the adsorption process and desorption process under different pressures was measured. The test results indicated that, at the same equilibrium pressure, the adsorption capacity during the desorption process was larger than that during the adsorption process, i.e., the desorption process exhibited hysteresis relative to the adsorption process.
- (3) The two-parameter equation of the Langmuir equation, the BET equation, and the D-R equation was used to fit and analyze the test results and the fitting parameters of the three equations were obtained. Comparing the correlation coefficients of the three equations, the order of fitting effect of the three equations to the gas adsorption of the bituminous coal was D-R equation > Langmuir equation > BET equation.
- (4) The permeability curves of the same coal sample to CH₄ and N₂ were nearly identical, while that of CO₂ was lower than those of the former two gases under the same conditions. The difference in the sorption characteristics of the three gases was considered the primary cause of the above permeability differences. The adsorption expansion effect of the coal matrix caused the squeezing of the porous coal masses, reducing their permeability.

6. Recommendation

The permeability and adsorption of the coal body are very critical parameters for the coal seam gas existing and gas extraction. This study tested the permeability of different components of coal seam gas, and the result shows that the permeability of CO₂ was found to be lower than that of other coal seam gas constituents. Then, in practical engineering applications, CO₂ can be injected into coal seams for gas replacement to improve the gas recovery rate and to grasp the gas gushing law at different stages. Alternatively, CO₂ can be injected into the strata for geological sequestration to reduce greenhouse gas emissions.

This study suggests injecting compressed air directly into the coal seam to promote continuous desorption by reducing the partial pressure of gas adsorption, increasing the pore pressure, reducing the effective stress in the coal body, maintaining the pore opening and thus promoting gas seepage, and finally releasing the gas from the coal seam continuously under the action of flow wrapping. Finally, it realizes the efficient extraction of coal seam gas.

Author Contributions: Conceptualization, G.W. and Z.Y.; validation, G.W., Z.Y. and L.Z.; formal analysis, Z.Y.; investigation, L.Z. and J.T.; data curation, G.W. and Z.Y.; writing—original draft preparation, G.W.; writing—review and editing, Z.Y., L.Z. and J.T.; funding acquisition, G.W., Z.Y. and L.Z. All authors have read and agreed to the published version of the manuscript.

Funding: This research was funded by the National Natural Science Foundation of China (52104167, 52174129), the Guizhou Provincial Key Technology R&D Program ([2023]337), Independent Research Project of State Key Laboratory of Coal Resources and Safe Mining, CUMT (SKLCRSM22X006).

Institutional Review Board Statement: Not applicable.

Informed Consent Statement: This study did not involve humans.

Data Availability Statement: The data used to support the findings of this study are available from the corresponding author upon request.

Acknowledgments: The authors gratefully acknowledge the financial support of the above organization.

Conflicts of Interest: The authors declare no conflict of interest.

References

1. Ranathunga, A.S.; Perera, M.S.A.; Ranjith, P.G.; Wei, C.H. An experimental investigation of applicability of CO₂ enhanced coal bed methane recovery to low rank coal. *Fuel* **2017**, *189*, 391–399. [[CrossRef](#)]
2. Moore, T.A. Coalbed methane: A review. *Int. J. Coal Geol.* **2012**, *101*, 36–81. [[CrossRef](#)]
3. Cai, J.; Hu, X.; Standnes, D.C.; You, L. An analytical model for spontaneous imbibition in fractal porous media including gravity. *Colloids Surf. A Physicochem. Eng. Asp.* **2012**, *414*, 228–233. [[CrossRef](#)]
4. Chen, X.; Liu, J.; Wang, L.; Qi, L. Influence of pore size distribution of different metamorphic grade of coal on adsorption constant. *J. China Coal Soc.* **2013**, *38*, 294–300.
5. Qi, L.; Wang, Z.; Yang, H. Research on the differences of the pore characteristics with different destroyed-type coals. *Adv. Mater. Res.* **2013**, *619*, 598–602. [[CrossRef](#)]
6. Cai, J.; Wei, W.; Hu, X.; Liu, R.; Wang, J. Fractal characterization of dynamic fracture network extension in porous media. *Fractals* **2017**, *25*, 1750023. [[CrossRef](#)]
7. Yang, H.; Wang, Z.; Ren, Z. Differences between competitive adsorption and replacement desorption of binary gases in coal and its replacement laws. *J. China Coal Soc.* **2015**, *40*, 1550–1554.
8. Krooss, B.; Bergen, F.; Gensterblum, Y.; Siemons, N.; Pagnier, H.; David, P. High-pressure methane and carbon dioxide adsorption on dry and moisture-equilibrated Pennsylvanian coals. *Int. J. Coal Geol.* **2002**, *51*, 69–92. [[CrossRef](#)]
9. Ottiger, S.; Pini, R.; Storti, G.; Mazzotti, M. Measuring and modeling the competitive adsorption of CO₂, CH₄, and N₂ on a dry coal. *Langmuir* **2008**, *24*, 9531–9540. [[CrossRef](#)]
10. Zhang, L.; Zhang, C.; Tu, S.; Tu, H.; Wang, C. A study of directional permeability and gas injection to flush coal seam gas testing apparatus and method. *Transp. Porous Media* **2016**, *111*, 573–589. [[CrossRef](#)]
11. Zhang, L.; Ye, Z.; Tang, J.; Hao, D.; Zhang, C. Comparative experiment study on nitrogen injection and free desorption of methane-rich bituminous coal under triaxial loading. *Arch. Min. Sci.* **2017**, *62*, 911–928. [[CrossRef](#)]
12. Yang, H.; Feng, C.; Chen, L. Mechanism Analysis on Experiment of Injecting Nitrogen to Displace Coal Seam Methane Under Different Pressure. *Saf. Coal Mines* **2017**, *48*, 145–148.
13. Shimada, S.; Li, H.; Oshima, Y.; Adachi, K. Displacement behavior of CH₄ adsorbed on coals by injecting pure CO₂, N₂, and CO₂-N₂ mixture. *Environ. Geol.* **2005**, *49*, 44–52. [[CrossRef](#)]
14. Harpalani, S.; Prusty, B.K.; Dutta, P. Methane/CO₂ sorption modeling for coalbed methane production and CO₂ sequestration. *Energy Fuels* **2006**, *20*, 1591–1599. [[CrossRef](#)]
15. Langmuir, I. The adsorption of gases on plane surfaces of glass, mica and platinum. *J. Am. Chem. Soc.* **1918**, *40*, 1361–1403. [[CrossRef](#)]
16. Lowell, S.; Shields, J.E. *Powder Surface Area and Porosity*; Chapman and Hall: London, UK, 1984; pp. 14–29.
17. Brunauer, S.; Deming, L.S.; Deming, W.E.; Teller, E. On a theory of the van der Waals adsorption of gases. *J. Am. Chem. Soc.* **1940**, *62*, 1723–1732. [[CrossRef](#)]
18. Sing, K.S. Adsorption methods for the characterization of porous materials. *Adv. Colloid Interface Sci.* **1998**, *76*, 3–11. [[CrossRef](#)]
19. Karacan, C.Ö.; Okandan, E. Assessment of energetic heterogeneity of coals for gas adsorption and its effect on mixture predictions for coalbed methane studies. *Fuel* **2000**, *79*, 1963–1974. [[CrossRef](#)]
20. Yang, R.T.; Saunders, J.T. Adsorption of gases on coals and heat-treated coals at elevated temperature and pressure: 1. Adsorption from hydrogen and methane as single gases. *Fuel* **1985**, *64*, 616–620. [[CrossRef](#)]
21. Weishauptová, Z.; Medek, J. Bound forms of methane in the porous system of coal. *Fuel* **1998**, *77*, 71–76. [[CrossRef](#)]
22. George, J.S.; Barakat, M.A. The change in effective stress associated with shrinkage from gas desorption in coal. *Int. J. Coal Geol.* **2001**, *45*, 105–113. [[CrossRef](#)]

23. Zhang, L.; Aziz, N.I.; Ren, T.; Nemcik, J.; Tu, S. Influence of coal particle size on coal adsorption and desorption characteristics. *Arch. Min. Sci.* **2014**, *59*, 807–820. [[CrossRef](#)]
24. Wang, Y.; Zhu, Y.; Liu, S.; Zhang, R. Methane adsorption measurements and modeling for organic-rich marine shale samples. *Fuel* **2016**, *172*, 301–309. [[CrossRef](#)]
25. Lin, H.; Huang, M.; Li, S.; Zhang, C.; Cheng, L. Numerical simulation of influence of Langmuir adsorption constant on gas drainage radius of drilling in coal seam. *Int. J. Min. Sci. Technol.* **2016**, *26*, 377–382. [[CrossRef](#)]
26. Qajar, A.; Daigle, H.; Prodanović, M. Methane dual-site adsorption in organic-rich shale-gas and coalbed systems. *Int. J. Coal Geol.* **2015**, *149*, 1–8. [[CrossRef](#)]
27. Busch, A.; Gensterblum, Y.; Krooss, B.M.; Siemons, N. Investigation of high-pressure selective adsorption/desorption behaviour of CO₂ and CH₄ on coals: An experimental study. *Int. J. Coal Geol.* **2006**, *66*, 53–68. [[CrossRef](#)]
28. Sakurovs, R.; Day, S.; Weir, S.; Duffy, G. Application of a modified Dubinin–Radushkevich equation to adsorption of gases by coals under supercritical conditions. *Energy Fuels* **2007**, *21*, 992–997. [[CrossRef](#)]
29. Tang, S.; Wan, Y.; Duan, L.; Xia, Z.; Zhang, S. Methane adsorption-induced coal swelling measured with an optical method. *Int. J. Min. Sci. Technol.* **2015**, *25*, 949–953. [[CrossRef](#)]
30. Day, S.; Duffy, G.; Sakurovs, R.; Weir, S. Effect of coal properties on CO₂ sorption capacity under supercritical conditions. *Int. J. Greenh. Gas Control* **2008**, *2*, 342–352. [[CrossRef](#)]
31. Fitzgerald, J.E.; Pan, Z.; Sudibandriyo, M.; Robinson Jr, R.L.; Gasem, K.A.M.; Reeves, S. Adsorption of methane, nitrogen, carbon dioxide and their mixtures on wet Tiffany coal. *Fuel* **2005**, *84*, 2351–2363. [[CrossRef](#)]
32. Busch, A.; Gensterblum, Y.; Krooss, B.M. Methane and CO₂ sorption and desorption measurements on dry Argonne premium coals: Pure components and mixtures. *Int. J. Coal Geol.* **2003**, *55*, 205–224. [[CrossRef](#)]
33. Chaback, J.J.; Morgan, D.; Yee, D. Sorption Irreversibilities and Mixture Compositional Behavior during Enhanced Coal Bed Methane Recovery Processes. In *SPE Gas Technology Symposium*; OnePetro: Richardson, TX, USA, 1996; p. SPE-35622-MS.
34. Karacan, C.Ö. Heterogeneous sorption and swelling in a confined and stressed coal during CO₂ injection. *Energy Fuels* **2003**, *17*, 1595–1608. [[CrossRef](#)]
35. Clarkson, C.R.; Bustin, R.M. Binary gas adsorption/desorption isotherms: Effect of moisture and coal composition upon carbon dioxide selectivity over methane. *Int. J. Coal Geol.* **2000**, *42*, 241–271. [[CrossRef](#)]
36. Dubinin, M.M. The Potential Theory of Adsorption of Gases and Vapors for Adsorbents with Energetically Nonuniform Surfaces. *Chem. Rev.* **1960**, *60*, 235–241. [[CrossRef](#)]
37. Harpalani, S.; Schraufnagel, R.A. Shrinkage of coal matrix with release of gas and its impact on permeability of coal. *Fuel* **1990**, *69*, 551–556. [[CrossRef](#)]

Disclaimer/Publisher’s Note: The statements, opinions and data contained in all publications are solely those of the individual author(s) and contributor(s) and not of MDPI and/or the editor(s). MDPI and/or the editor(s) disclaim responsibility for any injury to people or property resulting from any ideas, methods, instructions or products referred to in the content.